

Cytoplasmic maturation in human oocytes: an ultrastructural study†

Authors: Trebichalská, Z., Kyjovská, D., Kloudová, S., Otevřel, P., Hampl, A., et al.

Source: *Biology of Reproduction*, 104(1) : 106-116

Published By: Society for the Study of Reproduction

URL: <https://doi.org/10.1093/biolre/ioaa174>

The BioOne Digital Library (<https://bioone.org/>) provides worldwide distribution for more than 580 journals and eBooks from BioOne's community of over 150 nonprofit societies, research institutions, and university presses in the biological, ecological, and environmental sciences. The BioOne Digital Library encompasses the flagship aggregation BioOne Complete (<https://bioone.org/subscribe>), the BioOne Complete Archive (<https://bioone.org/archive>), and the BioOne eBooks program offerings ESA eBook Collection (<https://bioone.org/esa-ebooks>) and CSIRO Publishing BioSelect Collection (<https://bioone.org/csiro-ebooks>).

Your use of this PDF, the BioOne Digital Library, and all posted and associated content indicates your acceptance of BioOne's Terms of Use, available at www.bioone.org/terms-of-use.

Usage of BioOne Digital Library content is strictly limited to personal, educational, and non-commercial use. Commercial inquiries or rights and permissions requests should be directed to the individual publisher as copyright holder.

BioOne is an innovative nonprofit that sees sustainable scholarly publishing as an inherently collaborative enterprise connecting authors, nonprofit publishers, academic institutions, research libraries, and research funders in the common goal of maximizing access to critical research.

Research Article

Cytoplasmic maturation in human oocytes: an ultrastructural study[†]

Z. Trebichalská¹, D. Kyjovská², S. Kloudová², P. Otevřel², A. Hampl¹ and Z. Holubcová^{1,2,*}

¹Department of Histology and Embryology, Faculty of Medicine, Masaryk University, Brno, Czech Republic and

²Reprofit International, Clinic of Reproductive Medicine, Brno, Czech Republic

*Correspondence: Masaryk University Campus – building A1, Kamenice 3, 625 00 Brno, Czech Republic.

Tel: +420774006702; E-mail: zholub@med.muni.cz

[†]Grant Support: Grant Agency of the Czech Republic (GJ19-14990Y).

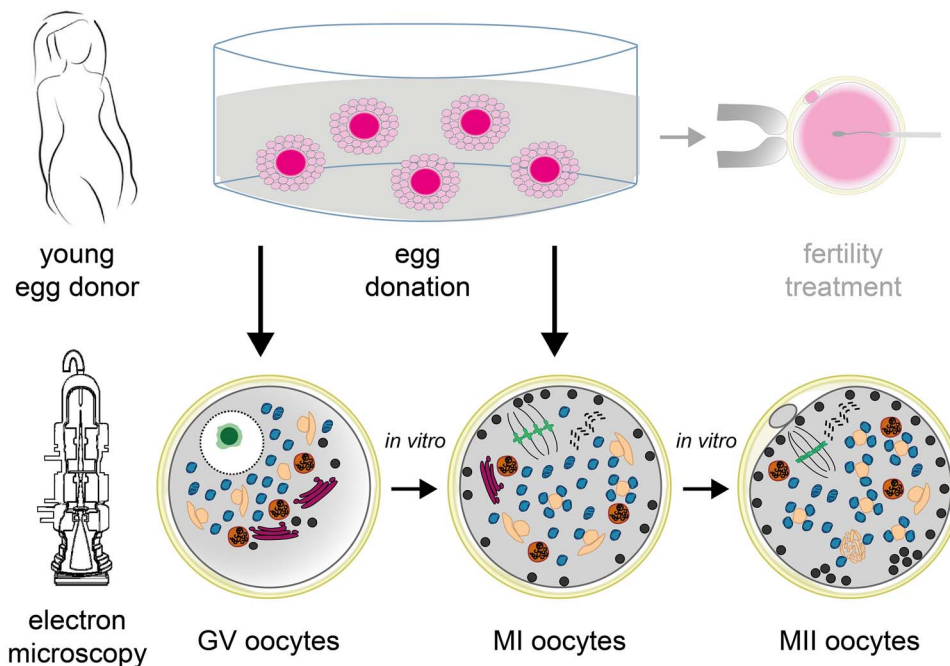
Received 14 July 2020; Revised 7 September 2020; Editorial Decision 15 September 2020; Accepted 15 September 2020

Abstract

Female fertility relies on successful egg development. Besides chromosome segregation, complex structural and biochemical changes in the cytoplasmic compartment are necessary to confer the female gamete the capacity to undergo normal fertilization and sustain embryonic development. Despite the profound impact on egg quality, morphological bases of cytoplasmic maturation remain largely unknown. Here, we report our findings from the ultrastructural analysis of 69 unfertilized human oocytes from 34 young and healthy egg donors. By comparison of samples fixed at three consecutive developmental stages, we explored how ooplasmic architecture changes during meiotic maturation in vitro. The morphometric image analysis supported observation that the major reorganization of cytoplasm occurs before polar body extrusion. The organelles initially concentrated around prophase nucleus were repositioned toward the periphery and evenly distributed throughout the ooplasm. As maturation progressed, distinct secretory apparatus appeared to transform into cortical granules that clustered underneath the oocyte's surface. The most prominent feature was the gradual formation of heterologous complexes composed of variable elements of endoplasmic reticulum and multiple mitochondria with primitive morphology. Based on the generated image dataset, we proposed a morphological map of cytoplasmic maturation, which may serve as a reference for future comparative studies. In conclusion, this work improves our understanding of human oocyte morphology, cytoplasmic maturation, and intracellular factors defining human egg quality. Although this analysis involved spare oocytes completing development in vitro, it provides essential insight into the enigmatic process by which human egg progenitors prepare for fertilization.

Summary Sentence: Ultrastructural characterization and morphometric analysis of maturing human oocytes reveal complex changes in cytoplasmic architecture that are associated with the acquisition of egg's developmental competence.

Graphical Abstract



Key words: human oocyte, in vitro maturation, cytoplasmic maturation, oocyte ultrastructure, electron microscopy, egg quality.

Introduction

The egg is a highly specialized cell uniquely equipped for a single function in the propagation of life. Its large cytoplasm contains a stockpile of cellular material needed to support embryonic metabolism upon fertilization [1–3]. Although the maternal influence on the embryonic fate is widely recognized, our understanding of egg biology remains rudimentary, especially in humans.

Oocyte maturation represents the final stage of oogenesis whereby a diploid oocyte produces a haploid egg. This process is induced by a hormonal surge triggering the resumption of meiosis in a prophase-arrested germinal vesicle (GV). This distinctive event is manifested as a germinal vesicle breakdown (GVBD) and followed by a transient stage during which a meiotic spindle assembles. The reduction division culminates with a metaphase I (MI) oocyte extruding half of the genetic material into a polar body (PB). Meiosis is again arrested in a metaphase of the second meiotic division (MII) when the mature oocyte is ovulated. Together with nuclear maturation, interrelated, yet less defined, cytoplasmic maturation must occur for production of the fertilizable egg. The complex structural and biochemical transformation of the oocyte cytoplasm is required to complete the second meiotic division, secure monospermic fertilization, and sustain early embryogenesis [4]. Female gametes are known to vary in their capacity to foster the development of a live offspring. In humans, egg quality is a limiting factor of reproduction success and efficiency of assisted reproduction techniques (ART) [5]. Cytoplasmic deficiency contributes to the low developmental capacity of embryos produced via in vitro maturation of ovarian follicles [6]. Experimentation in model species shed a light on cytoplasmic remodeling during mammalian egg development [7–10]. However, the extrapolation of animal data to humans is problematic due to interspecies differences in female gametogenesis.

Microscopy techniques proved to be an invaluable tool for research of scarce human oocytes. While fluorescent labeling enabled identification and tracking of specific structures of interest [11–15], electron microscopy is suited for visualization of the entire cytoplasmic content at the nanoscale level. Seminal electron microscopy studies disclosed peculiarities of human oocyte morphology, such as unconventional type of mitochondria and the absence of centrioles at the meiotic spindle [16–19]. However, they involved only a few failed-to-fertilize eggs or oocytes isolated from dissected ovaries of reproductively aged cancer patients and women undergoing surgery for gynecological disorders. Similarly, later work typically concerned spare aged and non-developing eggs from in vitro fertilization (IVF) cycles [20–22]. Therefore, whether all identified features also occur in good-quality oocytes is still unclear. Instead of investigating scientific principles underlying human oocyte development, current research focuses on addressing clinically relevant questions such as the impact of freezing and culturing protocols on the egg quality [23–26]. Previous studies reported organelle rearrangement in the ooplasm of developing mammalian oocytes [7–10]. However, in humans, the structural bases of cytoplasmic maturation have not been systematically researched.

This study was designed to re-evaluate current knowledge of cytoplasmic maturation by investigating the ultrastructural characteristics of human oocytes spontaneously maturing in vitro. In particular, we used transmission electron microscopy (TEM) to systematically analyze the subcellular morphology of samples individually fixed at three consecutive stages of meiotic maturation (GV, MI, MII). While most other studies utilized only a small number of eggs from patients seeking fertility treatment, we examined a representative number of freshly retrieved oocytes derived exclusively from young egg donors with no history of infertility.

Materials and methods

Source of oocytes

This study was conducted as a joint research activity with an academic (Department of Histology and Embryology, Faculty of Medicine, Masaryk University) and clinical laboratory (a single private IVF clinic Reprofit International). It involved an ultrastructural analysis of 69 surplus hormonally primed oocytes from 34 young women (aged 20–32 years, average 25.94 ± 3.18 years) who became actively recruited to enroll in egg donation program between September 2017 and October 2019. All participants showed an expected response to the superovulation-inducing regimen. Their mature eggs were used for fertility treatment, and left-over immature oocytes were donated for research. The study was undertaken under ethical approvals issued by the Ethics Committees of both collaborating institutions. Written informed consent was obtained from all participants.

Oocyte collection

Ovarian stimulation was induced with recombinant follicle-stimulating hormone (175 IU Gonalf, Merck Serono, Switzerland; Puregon, Organon, Netherlands). Pituitary suppression was achieved by administering the gonadotropin-releasing hormone antagonist (Orgalutran, Organon, Netherlands) starting when two 14 mm follicles were visualized in the ultrasound scan. When two or more follicles reached a diameter of 18 mm (in average 11.5 days of FSH administration), ovulation was induced by 0.2 mg triptorelin (Diphereline, Ipsen Pharma Biotech, France; Decapeptyl, Ferring Pharmaceuticals, Germany). Oocyte collection was scheduled 35–36 h after the triggering injection. The cumulus-oocyte complexes (COCs), retrieved from antral follicles larger than 12 mm using ultrasound-guided transvaginal aspiration, were collected in a MOPS/HEPES-buffered medium (#90166, MHM-C, Irvine Scientific, USA). The oocyte denudation was undertaken 10 min after retrieval. The COCs were briefly exposed to hyaluronidase (#90101, Irvine Scientific, USA), and cumulus-corona cells were mechanically removed by gentle pipetting. The meiotic status of each oocyte was determined based on the presence/absence of the prophase nucleus/first PB observed in transmitted light (Nikon Eclipse TE 2000-U microscope, Tokyo, Japan). The oocytes, unsuitable for fertility treatment because of their immaturity at the time of ICSI, were donated for research provided that informed consent was obtained. Prior to fixation, the late-maturing oocytes were incubated in a Continuous Single Culture medium (#90165, CSCM, Irvine Scientific, USA) covered with mineral oil and a humidified atmosphere of 5% O₂ and 6% CO₂ until they reached a distinctive developmental stage of oocyte maturation (GV oocytes 1–3 h; close-to-anaphase MI oocytes 4–6 h, MII-arrested oocytes 6–24 h). The presence of MI/MII spindle was confirmed by polarized light microscopy (OCTAX polarAIDE™, MTG, Germany), as described previously [27]. The morphology of each oocyte was evaluated by an experienced clinical embryologist, and overall appearance was photographed for documentation purposes. Oocytes that failed to complete maturation in the expected time, as well as those displaying any type of dysmorphism, were excluded from the study.

Electron microscopy

The chemical fixation of oocytes was carried out in 3% glutaraldehyde (Agar Scientific, Stansted, UK) in 0.1 M sodium cacodylate buffer (Sigma Aldrich, St. Louis, USA) (pH 7.2–7.8) supplemented

with 1% tannic acid (Sigma Aldrich, St. Louis, USA) at room temperature. Following overnight immersion, the samples were rinsed in 0.1 M sodium cacodylate buffer and postfixed in 1% osmium tetroxide (Sigma Aldrich, St. Louis, USA) in 0.1 M sodium cacodylate buffer supplemented with 1.5% potassium ferrocyanide (Sigma Aldrich, St. Louis, USA). The individual oocytes were embedded in a block of 3% agarose (Sigma Aldrich, St. Louis, USA), dehydrated in graded series of ethanol and pure acetone (Penta Chemicals, Prague, Czech Republic), passed through two baths containing acetone and epoxy resin (Sigma Aldrich, St. Louis, USA) at the proportion 1:1 and 1:3 and finally embedded into pure epoxy resin. The block of hardened sample-containing resin was serially sectioned using ultramicrotome Leica EZ4 equipped with a diamond knife. The ultrathin sections (60–70 nm) were mounted on nickel and copper grids and poststained with 1% aqueous uranyl acetate (Agar Scientific, Stansted, UK) and 3% lead citrate (Sigma Aldrich, St. Louis, USA). TEM sections were inspected at the FEI Morgagni 268D microscope.

Image analysis

The diameter of each oocyte and width of the Zona Pellucida (ZP) were measured from transmitted light images of live oocytes photographed before fixation. Three diameter/ZP measurements were performed in each cell and averaged. The total/categorical morphometric data and donor age distribution were expressed as arithmetic means \pm standard deviation (SD). The density of organelles (number of particles per 10 μm^2) was measured using particle analysis function (Fiji software [28]) in binarized cross-sectional micrographs of 15 oocytes (5 oocytes representing each developmental category) imaged under identical microscope settings. Only particles greater than 0.05 μm^2 in TEM images with 2200 \times magnification were counted. The comparison of organelle density in the central versus cortical area (one box in the central area and one box 10 μm underneath the oolema) was performed in three TEM sections of each oocyte and averaged. The data showing arithmetic means \pm standard deviation (SD) were plotted. Statistical significance was evaluated by one-way analysis of variance (ANOVA, Excel) with p -value < 0.001 regarded as a significant difference.

Results

Sample characteristics

An ultrastructural analysis involved a total of 69 surplus oocytes recovered from large antral follicles of young egg donors. The donated immature oocytes were either fixed at the same development stage as observed at retrieval (GV, MI) or kept in culture to complete the maturation process before fixation (72% MII oocytes were derived from GV oocytes). Based on a standard morphological assessment combined with noninvasive spindle imaging, the collected samples were assigned into three categories corresponding to distinct maturation stages: (1) the GV oocytes (25 samples), (2) MI oocytes (19 samples), and (3) mature MII oocytes (25 samples). The majority of collected GV oocytes (77.78%) exhibited eccentric nuclei suggestive of their advanced prophase stage [29]. The MI oocytes were cultured until they developed an MI spindle signal detectable by polarized light microscopy. The presence of spindle birefringence indicated that these oocytes already progressed through the first meiotic division and were about to extrude PB. The completion of the maturation was confirmed by the detection of a bipolar MII

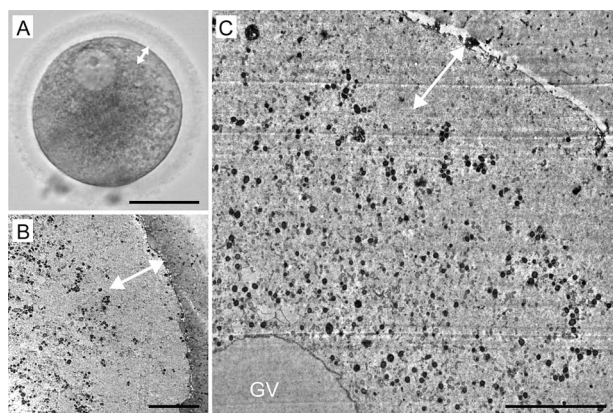


Figure 1. A representative example of human germinal vesicle (GV) oocyte morphology: live appearance in transmitted light (A) and TEM micrographs (B, C). The cortical halo (double head arrow) corresponds to the area deprived of detectable organelles. Scale bar, 50 μm (A) and 10 μm (B, C).

spindle in PB-positive oocytes (Supplementary Figure 1). The fixation of morphologically normal oocytes was performed at specific time points of maturational program to curtail the inherent heterogeneity of the studied cell type. As documented in Supplementary table, there were no significant differences in basic morphometric parameters (oocyte diameter, the width of Zona Pellucida) and egg age distribution among developmental subcategories. These data indicated that the analyzed sample set is relatively uniform, and the observed differences in the ultrastructure represent the morphological changes associated with the progression through the meiotic program.

Ultrastructural features

Using electron microscopy, we inspected fine ultrastructural details of individual organelles, their physical interactions, and overall distribution within the cytoplasm in individual oocytes. For clarity and continuity, the morphological observations are presented in the context of oocyte's progression through maturation.

Distribution of organelles. In all GV oocytes, detectable organelles displayed non-homogenous distribution throughout the cytoplasm. The subcellular structures were concentrated in the perinuclear region, whereas the cytoplasm underneath the oolema appeared to be devoid of organelles. The “organelle-free” cortical area was usually so prominent that it could be seen even in the optical microscope in the form of a light halo, which disappears as the oocyte re-enters meiosis (Figure 1). On the contrary, in spindle-positive MI and MII oocytes, the organelles were dispersed homogeneously throughout the entire volume of the cell except in the meiotic spindle territory (Figure 2 and Figure 3). Unlike authors of previous mouse oocyte studies [30–32], we observed no evident polarization of the ooplasm or accumulation of organelles in the vicinity of the chromosome-spindle mass (Figure 2B and Figure 3B). The particle analysis in cross-section micrographs of oocytes fixed at three maturational stages has shown that the periphery (10 μm from oolema) to center ratio of organelle density was significantly lower ($p < 0.001$) in GV oocytes (0.43 ± 0.15), than in MI and MII oocytes (0.94 ± 0.19 and 0.97 ± 0.03 , respectively) (Figure 4). This result indicates that the major relocalization of organelles occurs during the transition from prophase to metaphase of the first meiotic division.

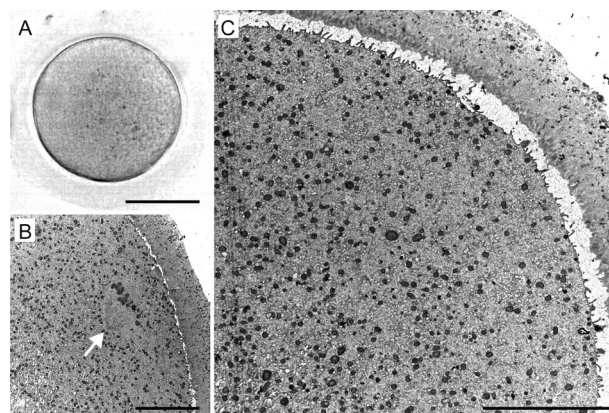


Figure 2. A representative example of human metaphase I (MI) oocyte morphology: live appearance in transmitted light (A) and TEM micrographs (B, C). The organelles are evenly distributed in the ooplasm (B, C), and the metaphase I spindle (arrow) is oriented perpendicularly to the surface (B). Scale bar, 50 μm (A) and 10 μm (B, C).

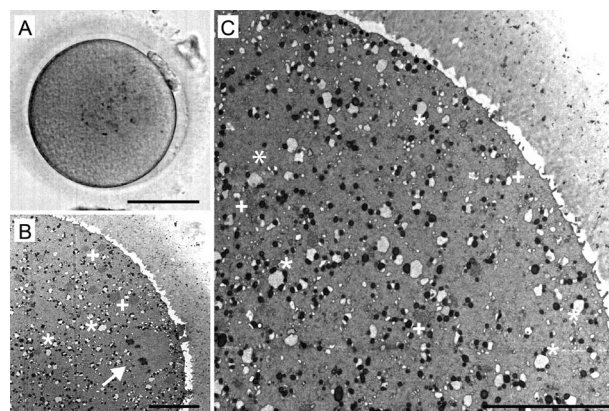


Figure 3. A representative example of human metaphase II (MII) oocyte morphology: live appearance in transmitted light (A) and TEM micrographs (B, C). The characteristic “necklace-like” complexes of mitochondria and endoplasmic reticulum (ER) (*), as well as large aggregates of tubular ER (+), are visible in the cytoplasm (B, C) and the metaphase II spindle (arrow) is oriented perpendicularly to the surface (B). Scale bar, 50 μm (A) and 10 μm (B, C).

Nuclear complement. The remarkably large prophase nuclei of GV oocytes ($29.06 \pm 1.63 \mu\text{m}$ in diameter) were found to contain compact electron-dense nucleoli and an associated mass of chromatin showing different degrees of condensation. The spherical GV was confined by a nuclear envelope with the distinctive pores (Figure 5A–C). In several analyzed oocytes, the nuclear outline appeared slightly undulated, suggesting that it had faced an osmotic pressure during sample immersion in fixative. Five oocytes (derived from two donors), which were assigned to the GV category after collection, underwent GVBD shortly before fixation. Here, the nuclear domain collapsed, and cytoplasmic compounds penetrated the area. Nucleolus opacity diminished while the nuclear envelope became highly infolded and appeared to dismantle. Fragments of the nuclear membrane were found in the form of tightly packed laminar arrays, termed as the annulate lamellae (Figure 5D–F) [16].

In MI and MII oocytes, the meiotic spindle was detected close to the oolema. As previously reported [16, 19, 33], the human oocyte spindle was found to be relatively short, barrel-shaped, anastral, and

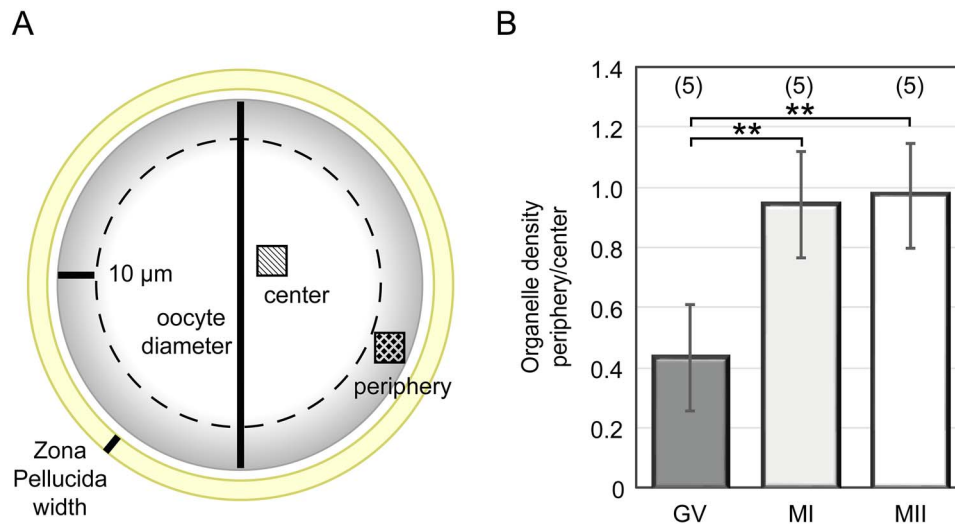


Figure 4. The morphometric analysis of organelle distribution in the cytoplasmic compartment of maturing human oocytes. The organelle density in the periphery versus central area of individual cells was compared (A), the average ratio was calculated in individual GV, MI, and MII oocytes and plotted for developmental categories (B). The number of analyzed oocytes is stated in brackets. *p-value < 0.001.

perpendicularly oriented toward the cell surface. Genetic material was visible in the form of bivalent chromosomes (MI oocytes) or a pair of sister chromatids (MII oocytes), mostly aligned in the equatorial plate of the spindle (Figure 5G, H). As shown in Figure 3B and Figure 5H, the oolema overlying MII spindle was covered by numerous protrusions, which contrasts to the presence of a microvilli-free area in mouse oocytes [34]. Even though we repeatedly performed serial sectioning of randomly positioned oocyte spindles, no centrioles were detected at poles where microtubule fibers converged (Figure 5G–I). This negative result is in agreement with previous findings that, in human oocytes, the meiotic spindle is assembled in the absence of typical centrosomes [11].

Cytoplasmic compartment. The cytoplasmic organelles detectable in our samples were mainly represented by mitochondria, endoplasmic reticulum (ER), and Golgi apparatus (GA). The most abundant organelles in oocytes of all maturational stages were the mitochondria. They were remarkably small ($0.3\text{--}0.7\ \mu\text{m}$; average diameter $448.99 \pm 12.26\ \text{nm}$) and did not exhibit conventional morphology found in somatic cells. Instead of rod-shaped organelles with a typically wrinkled inner membrane, human oocytes featured round-to-oval mitochondria with a dense matrix and sparse, either parallel or transversal, cristae (Figure 6A–C). The incidence of the former and latter category of these “oocyte-type” mitochondria was estimated at 3 to 1. The morphology of the mitochondria, as well as their number, did not seem to change dramatically during meiotic maturation. However, we registered maturation-related alteration of mitochondrial microtopography. Before GVBD, the individual mitochondria and small mitochondrial clusters were concentrated in the perinuclear area and absent from the outer part of the cytoplasm (Figure 1B, C). In MI oocytes, the numerous mitochondria populated the cortical region and showed a tendency to approach randomly distributed ER structures (Figure 2B, C; Figure 6D–F). The pleiomorphic ER was present in the form of isolated sacs, multivesicular complexes, elongated cisterns, or aggregates of short tubular membrane systems (Figure 6E–I). Notably, individual ribosomes, polyribosomal complexes, or rough ER were not readily detectable in our TEM images. Comparison of GV, MI, and MII oocytes indicated that the gradual affiliation

of the mitochondria to a smooth membrane of variable ER elements, occurring in MI oocytes, precedes the emergence of larger mitochondria-ER complexes (Figure 2B, C; Figure 6D–I). In mature oocytes, most mitochondria were already physically associated with ER membranes. Their ooplasm exhibited characteristic “necklace-like” [16, 19] complexes composed of a spherical sac decorated with circularly arranged mitochondria (Figure 6E, F). Besides these relatively small complexes ($1.75 \pm 0.49\ \mu\text{m}$), larger ($2.75 \pm 0.53\ \mu\text{m}$) tubular aggregates of ER surrounded by several mitochondria were common at the periphery of MII-arrested oocytes but not immature oocytes (Figure 6G–I). This observation suggests that they might represent the most advanced stage of mitochondria-ER conglomeration. Surprisingly, ultrastructural analysis of two normal-looking oocytes from one donor revealed extremely enlarged patches ($4.74 \pm 1.18\ \mu\text{m}$ in diameter) of tightly packed tubules associated with only a few mitochondria. These voluminous aggregates were typically located in the cortical area and surrounded by cytoplasm, which was deprived of detectable organelles. The described anomaly in organelle distribution raises concerns about the developmental competence of affected oocytes.

Distinct GA, composed of an interconnected system of cisternae and vesicles, was regularly found only in the cytoplasm of GV oocytes (Figure 7A, B). However, unlike in somatic cells, the cis-trans polarity of GA was not easily distinguishable here. The GA remnants were occasionally detected in MI oocytes but never in MII oocytes (Figure 7C). This observation supports the notion that GA undergoes progressive disintegration in the course of maturation. Cortical granules (CGs), characteristic for unfertilized oocytes, are known to be derived from GA [35, 36]. We observed numerous small ($0.3\text{--}0.4\ \mu\text{m}$ in diameter) electron-dense vesicles underneath the oolema of close-to-anaphase MI oocytes as well as MII-arrested oocytes (Figure 7D–F). On the contrary, only a few isolated CGs were detected in the cortical area of GV oocytes (Figure 1B). Unlike in mouse oocytes, in which the area around the meiotic spindle was shown to be CGs-free [37], in human oocytes, CGs were docked even under the oolema overlying the MII spindle (Figure 5H). The diverse signal intensity of granules within the same oocyte opens the question regarding variability in content and the biological function of different subpopulations of these vesicles (Figure 7D–F).

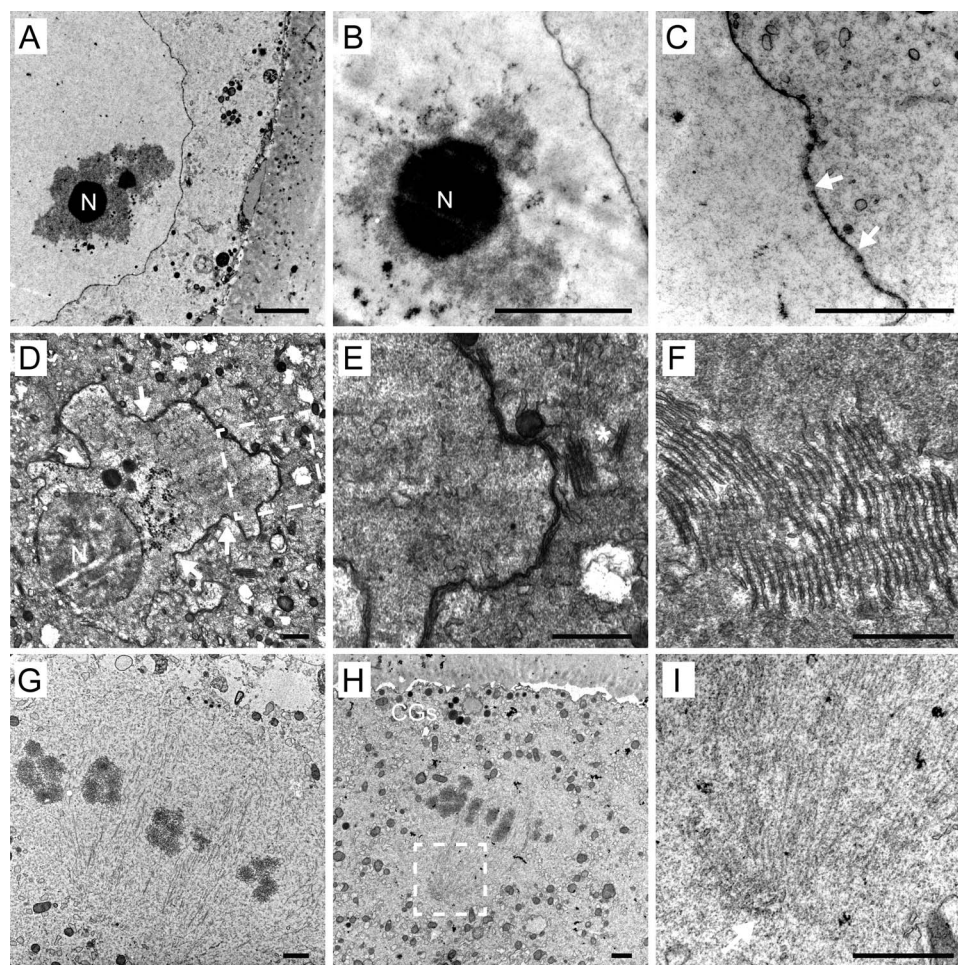


Figure 5. Nuclear area of germinal vesicle (GV) oocytes (A–C) and oocytes undergoing germinal vesicle breakdown (GVBD) (D–F): An overview (A) and detail (B) of GV with nucleolus (N) surrounded by chromatin exhibiting different degrees of compaction. Detail of nuclear envelope with distinct nuclear pores (arrows) (C). An overview (D) of the collapsing nuclear area with the infolded nuclear envelope (arrows) and nucleolus (N) in GVBD oocyte. A magnified image (dashed rectangle in D) of the dismantling nuclear envelope (E) with an adjacent stack of membrane fragments (*). Detail of the annulate lamellae composed of membrane fragments forming lamellar arrays (F). Meiotic spindle area (G–I): Microtubule fibres and chromosomes aligned at metaphase are visible (G, H). The cortical granules (CGs) and membrane protrusions are present in the area overlaying the spindle (H). Detail of the spindle pole (dashed rectangle in H) lacking centrioles at the site of microtubule convergence (arrow) (I). Scale bar, 1 μm (A, B, D–I); 500 nm (C).

Like mitochondria, the lysosomes were found in the cytoplasm of all analyzed oocytes. They varied in size (0.2–1.5 μm) and ultrastructural appearance. Some of them were noticeable under low magnification as dark refractile specks disrupting cytoplasm homogeneity. Such cytoplasmic inclusions are commonly referred to as refractile bodies due to their autofluorescence [38]. Electron microscopy showed that these structures were membrane-bound bodies containing residues of lysosomal degradation. In accordance with their biological role of accumulation and disposal of waste material, lysosomes adopted the form of membrane-bound bodies containing aggregated vesicles with variable opacity, membrane remnants, or dark, dense patches, which might correspond to insoluble lipid droplets (Figure 7G–I). On the contrary, no signs of vacuolization or mitochondrial swelling were observed in our samples.

Discussion

Due to prevailing ethical and technical issues, the human egg biology is notoriously understudied. The scientific data about the fine

morphology of human oocytes are limited and scattered in the literature. Here, we used electron microscopy as a tool to study the structural basis of the cytoplasmic maturation, which renders the female gamete competent for postfertilization development. To this end, we examined the ultrastructure of preovulatory human oocytes spontaneously maturing *in vitro* and mapped out spatio-temporal rearrangements of organelles during meiotic maturation.

The strength of the study is the unprecedented sample quality and size of the cohort. Altogether, we inspected over 1500 TEM sections from 69 donor oocytes fixed at three defined stages of maturation. The egg progenitors we studied were retrieved in stimulated ART cycles but were rejected for an IVF procedure due to their immaturity at the time of insemination. Given that these oocytes failed to respond adequately to hormonal trigger and their maturation *in vitro* took place at in the absence of surrounding granulosa cells, there is a possibility that they differ from *in vivo* ovulated eggs. The fertilization and developmental potential of late-maturing oocytes were shown to be compromised, nevertheless they are still capable of producing live offspring [39–42]. Importantly, the

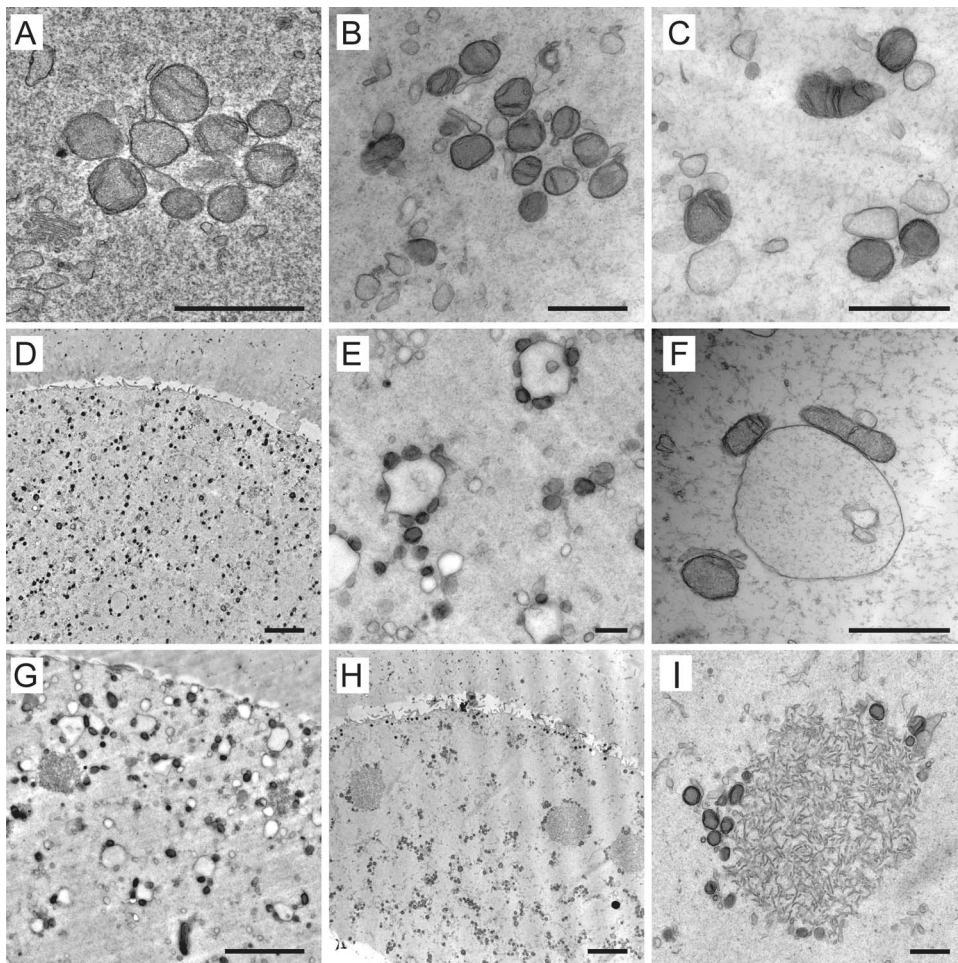


Figure 6. Examples of mitochondria and endoplasmic reticulum (ER) arrangements in human oocytes. The atypical mitochondria with transversal or arc-like cristae forming small clusters in immature oocytes (A–C). Overview (D, G, H) and details (E, F, I) of the mitochondria-ER complexes in mature oocytes. Besides characteristic “necklace-like” complexes formed by variable-sized sacs of ER decorated by several mitochondria (E, F), enlarged tubular aggregates of ER surrounded by only a few mitochondria could be found also in metaphase II oocytes (G–I). Scale bar, 1 μm (A, B, C, E, F, I) and 5 μm (D, G, H).

immature human oocytes included in this study have been provided exclusively by young egg donors tested for genetic and medical factors compromising fertility. Thus, the impact of major factors adversely affecting oocyte quality, namely maternal age and individual (in)fertility background, was substantially mitigated. Due to the relative homogeneity of the study population, time-specific fixation, and consistent processing of samples, the documented morphological patterns for each developmental stage were highly reproducible. Although the effect of hormonal stimulation and *in vitro* culture on the efficiency of oocyte maturation cannot be excluded, the samples examined here are of better biological quality than those commonly used in human oocyte studies.

Notably, our ultrastructural findings add to existing evidence that there are remarkable morphological differences between human sex cells and their mouse counterparts [33, 43]. Disparities, such as clustering of organelles in the perinuclear area, gradual formation of mitochondria ER complexes, absence of organelle aggregation around the meiotic spindle, and no microvilli/CGs-free zone underneath the oolema, are likely to reflect interspecies variations in biochemistry and physiology of reproduction. In the light of these observations, scientific data obtained from experiments in model organisms need to be interpreted with caution and, if possible,

verified in humans. The spare immature oocytes, usually discarded in IVF clinics, represent a pool of experimental material suitable to investigate human-specific aspects of egg biology.

The rigorous analysis of our large collection of micrographs of maturing human oocytes and a review of previously published ultrastructural reports enabled us to draw a timeline of morphological changes underlying the final stage of egg development (Figure 8). Based on the TEM data, the major structural features of human oocyte maturation involve (1) accumulation of organelles around prophase nucleus, (2) collapse of nuclear domain and fragmentation of the nuclear envelope at GVBD, (3) organelle dispersion toward the periphery of the oocyte during meiosis I, (4) progressive disintegration of GA accompanied by deposition of CGs in subcortical area, and (5) gradual arrangement of variable ER and mitochondria complexes. The characteristic ultrastructural patterns of each stage could serve as a reference for future studies assessing the effect of the patient’s medical background, stimulation protocol, or *in vitro* culture conditions. However, the fixed cell images represent snapshots of a dynamic process. Therefore, live-imaging strategies must be employed to validate proposed organelle interactions.

The uneven distribution of organelles we observed in GV oocytes has a parallel in pronuclear human zygotes. Here, the organelle

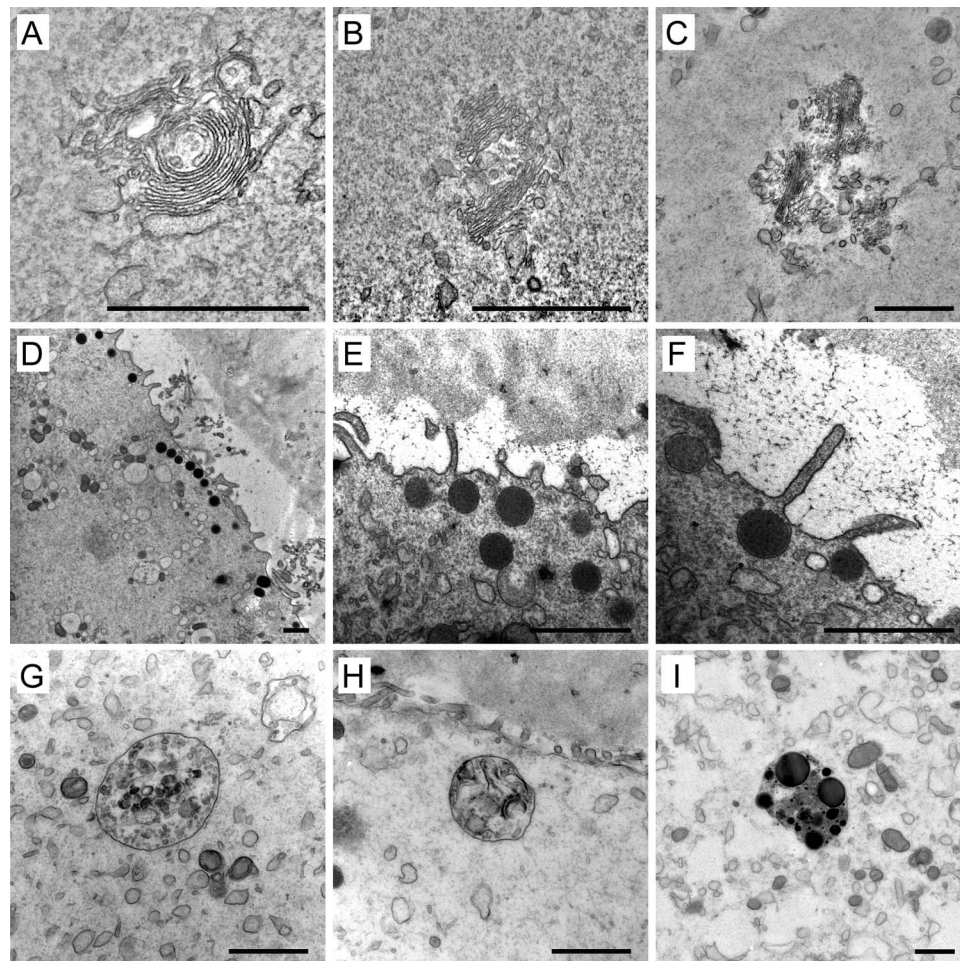


Figure 7. Examples of the Golgi apparatus (GA) (A–C), cortical granules (CGs) (D–F), and lysosomes (G–I) in human oocytes. The complex structure of GA in immature oocytes (A, B) and remnants of the secretory apparatus in a mature oocyte (C). Overview of clusters (D) and detailed morphology (E, F) of CGs stored underneath the oolema. Membrane-bound bodies containing small vesicles (G), remnants of membranes (H), and lipid droplets (I). Scale bar, 1 μm.

paucity in the subcortical region manifests as a “zygotic halo” [44]. The increased organelle density is supposed to support resource and energy supply for metabolically active haploid nuclei during the meiosis-to-mitosis transition. Analogously, the concentration of organelles around GV might be required to meet the high energetical demand of prophase nucleus anticipating the resumption of meiosis. The perinuclear conglomeration of organelles poses a challenge for experimental GV and pronuclear transfer procedures developed to avoid transmission of mitochondrial diseases [45–47].

The global maturation-induced redistribution of organelles is accompanied by their morphological adaptations that appear to be involved in the production and storage of substances or membranes vital for embryo development. For instance, the annulate lamellae observed at the vicinity of the collapsing GV might serve as a reservoir of membrane fragments for reassembly of the nuclear envelope after fertilization. Similarly, the multipurpose secretory apparatus transforms into secretory vesicles with a specific function in reproduction. Although the process of CGs budding was not directly evidenced in our images, the observation that the disintegration of GA coincides with the emergence of CGs supports the concept of progressive developmental specialization during female gametogenesis. Mitochondrial remodeling during oocyte maturation involves their rearrangement rather than a change in total numbers or internal

morphology. Organelle aggregation during spontaneous maturation was found to increase mitochondrial activity in mouse oocytes [32]. In human oocytes, no coalescence of organelles was observed around the forming meiotic spindles. Instead, the mitochondrial population formed characteristic complexes with ER, which serves as the primary storage for intracellular calcium (Ca^{2+}) [48]. The close association of ER with multiple energy-producing organelles facilitates an adequate response to the oocyte-activating stimulus delivered by the sperm at the time of fertilization. The functional basis for the morphological differences between clusters containing either vesicular or tubular type ER (sometimes called M-V and M-SER complexes, respectively [18, 21]) are not known and deserve to be investigated. However, it is tempting to speculate that, in the enlarged aggregates composed of ER tubules, surrounded by only a few mitochondria, the effectiveness of Ca^{2+} management might be compromised, thus diminishing the fertilization potential of the affected egg. This notion is in line with the observation of extremely voluminous ER clusters in poor-quality oocytes derived from infertile patients [49]. Detection of this ultrastructural aberration in oocytes exhibiting normal appearance under an optical microscope denotes that routine morphological inspection performed in clinical laboratories provides only limited information about the intrinsic quality of the egg.

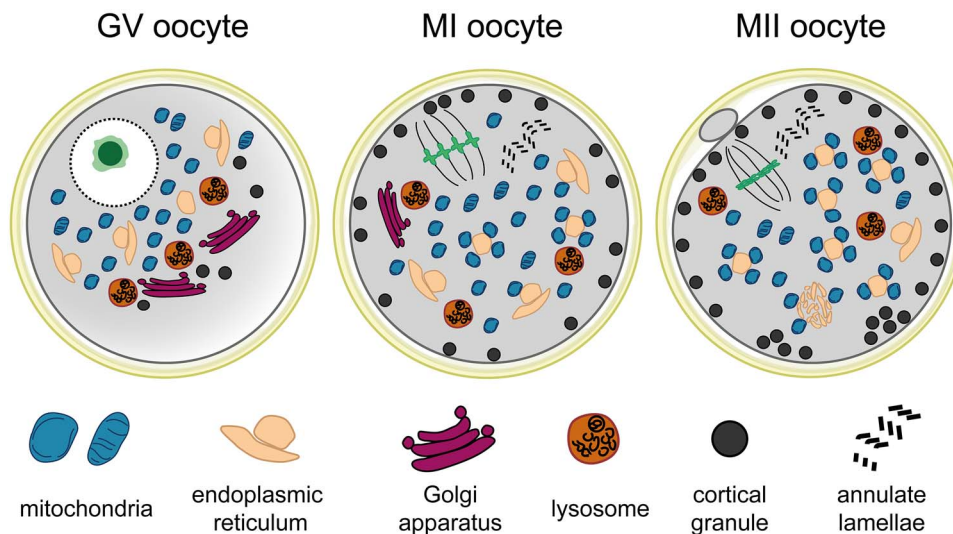


Figure 8. The schematic representation of subcellular morphological patterns in germinal vesicle (GV), metaphase I (MI) and metaphase II (MII) oocytes.

The function of the organelle is intimately intertwined with its internal structure. Our inspection of a large number of TEM micrographs confirmed previous findings that human oocytes house mitochondria with unique characteristics [16–19]. The population of simple mitochondria with a spherical or ovoid shape and spare arched-like cristae was uniformly found in all inspected oocytes representing three different stages of maturation. This “primitive” architecture is in contrast to the tubulo-vesicular profile seen in primordial germ cells and oogonia, lamellar type observed in egg progenitors entering meiotic prophase, and elongated mitochondria with numerous transversal cristae present in somatic cells [50]. It would be interesting to investigate whether interference with the balance of mitochondrial fusion and fission [51] would result in a change of organelle morphological pattern and/or mitochondrial quality control during oogenesis. The extraordinary arrangement of the mitochondrial membrane raises questions regarding the effectiveness of oxidative phosphorylation in human oocytes. In the absence of inner mitochondrial membrane invaginations, the surface area for aerobic respiration is severely reduced. The experiments in model systems demonstrated that DNA transcription, electron transport, and free radical production are suppressed in female gametes [52]. Based on these results, it has been suggested that the quiescent state of primitive mitochondria might avoid the incremental accumulation of reactive oxygen species produced by the respiratory chain. Preventing DNA and cellular damage caused by by-products of aerobic respiration is particularly important for long-living cells such as oocytes. The silencing of mitochondrial metabolism in the female germline might constitute the mechanism for increasing fidelity of mitochondrial inheritance [52]. Upon fertilization, transcriptionally and bioenergetically suppressed mitochondria are gradually replaced by the somatic type of mitochondria, which is concomitant with increased utilization of glucose [53–56]. Interestingly, the same type of atypical mitochondria are present in naïve pluripotent stem cells but vanish after differentiation [57, 58].

Although traditionally employed to study human oocyte morphology, TEM has critical technical limitations that have to be considered to avoid misconceptions. Our protocol was optimized to provide ultrastructural details described in the previous studies [17, 25, 33, 36]. It proved sufficient to sustain the fibrillar

structure of microtubule bundles within the meiotic spindle but not actin microfilaments forming a dense network within large female gametes [59–61]. Notably, the paucity of TEM-detectable ribosomes, reported by us and others [19, 20, 33, 36], is in sharp contrast with the well-documented translational activity of maturing oocytes [11, 50, 62–64]. We are speculating that these minute, non-membranous organelles might be particularly susceptible to dissolution in organic solvents used in electron microscopy protocols. Better fixation techniques are needed to prevent the disintegration of delicate structures critical for fundamental biological processes such as vesicle trafficking and proteosynthesis. Particularly, the cryo-electron microscopy holds the potential to preserve cells in a close-to-native-state and avoid unwanted artifacts [65]. Importantly, when interpreting TEM observations, it is necessary to acknowledge that two-dimensional micrographs provide only incomplete information about the spatial arrangement of subcellular components in large oocyte volume. Current methodological advances in volumetric imaging provide the opportunity to investigate oocyte morphology in three dimensions [66]. Comprehension of the complexity of the organization of the ooplasm and the precise quantification of organelles are necessary for further development of methods involving the transfer of cytoplasm or nuclear material to avoid mitochondrial diseases or “rejuvenate” reproductively aged oocytes [67].

In conclusion, this study enhances our knowledge of the fine morphology of human oocytes and helps to elucidate structural bases of cytoplasmic maturation. The fact that this ultrastructural analysis was performed on the representative number of good quality oocytes from young egg donors makes our findings highly informative of the biological process by which the egg acquires developmental competence. Our observations raise questions regarding the functional significance of organelle rearrangements in preparation for fertilization and the morphological factors defining the quality of the human egg. We hope to encourage studies that would combine the power of high-resolution and live-cell microscopy to advance our understanding of the cell which stands at the beginning of our lives.

Supplementary material

Supplementary material is available at *BIOLOGICAL REPRODUCTION* online.

Acknowledgments

The authors wish to thank the staff of Reprofit International for their kind assistance in the recruitment of egg donors and collecting informed consent. We gratefully acknowledge Assoc. Prof. Miroslava Sedláčková for her help with the interpretation of TEM images and critical review of the manuscript.

Conflict of interest

All authors declare no conflict of interest.

Funding

This study was funded by Grant Agency of the Czech Republic (GJ19-14990Y).

Author contribution

Z.T. carried out sample processing, electron microscopy, data analysis and interpretation, and manuscript and figure drafting; D.K. performed the sample collection, morphological assessment, and sample fixation; S.K. contributed toward informed consent collection and archive, and manuscript critical reading; P.O. contributed toward recruitment and hormonal stimulation of egg donors, and manuscript critical reading; A.H. carried out the revision and final approval of manuscript; Z.H. performed project design, data analysis, and interpretation, and manuscript writing. All authors discussed the results and commented on the final manuscript.

References

1. Stitzel ML, Seydoux G. Regulation of the oocyte-to-zygote transition. *Science* 2007; 316:407–408.
2. Mtango NR, Potireddy S, Latham KE. Oocyte quality and maternal control of development. *Int Rev Cell Mol Biol* 2008; 268:223–290.
3. Lu X, Gao Z, Qin D, Li L. A maternal functional module in the mammalian oocyte-to-embryo transition. *Trends Mol Med* 2017; 23:1014–1023.
4. Cotichio G, Dal Canto M, Mignini Renzini M, Guglielmo MC, Brambillasca F, Turchi D, Novara PV, Fadini R. Oocyte maturation: Gamete-somatic cells interactions, meiotic resumption, cytoskeletal dynamics and cytoplasmic reorganization. *Hum Reprod Update* 2015; 21:427–454.
5. Rienzi L, Balaban B, Ebner T, Mandelbaum J. The oocyte. *Hum Reprod* 2012; 27:i2–i21.
6. Watson AJ. Oocyte cytoplasmic maturation: A key mediator of oocyte and embryo developmental competence. *J Anim Sci* 2007; 85:E1–E3.
7. Kline D. Attributes and dynamics of the endoplasmic reticulum in mammalian eggs. *Curr Top Dev Biol* 2000; 50:125–154.
8. Brevini TA, Cillo F, Antonini S, Gandolfi F. Cytoplasmic remodelling and the acquisition of developmental competence in pig oocytes. *Anim Reprod Sci* 2007; 98:23–38.
9. Ferreira EM, Vireque AA, Adona PR, Meirelles FV, Ferriani RA, Navarro PA. Cytoplasmic maturation of bovine oocytes: Structural and biochemical modifications and acquisition of developmental competence. *Theriogenology* 2009; 71:836–848.
10. Mao L, Lou H, Lou Y, Wang N, Jin F. Behaviour of cytoplasmic organelles and cytoskeleton during oocyte maturation. *Reprod Biomed Online* 2014; 28:284–299.
11. Holubcová Z, Blayney M, Elder K, Schuh M. Human oocytes. Error-prone chromosome-mediated spindle assembly favors chromosome segregation defects in human oocytes. *Science* 2015; 348:1143–1147.
12. Sakakibara Y, Hashimoto S, Nakaoka Y, Kouznetsova A, Höög C, Kitajima TS. Bivalent separation into univalents precedes age-related meiosis I errors in oocytes. *Nat Commun* 2015; 6:7550.
13. Zielinska AP, Holubcová Z, Blayney M, Elder K, Schuh M. Sister kinetochore splitting and precocious disintegration of bivalents could explain the maternal age effect. *Elife* 2015; 4:e11389.
14. Gruhn JR, Zielinska AP, Shukla V, Blanshard R, Capalbo A, Cimadomo D, Nikiforov D, Chi-Ho Chan A, Newnham LJ, Vogel I, Scarica C, Krapchev M et al. Chromosome errors in human eggs shape natural fertility over reproductive life span. *Science* 2019; 365:1466–1469.
15. Roeles J, Tsiavaliaris G. Actin-microtubule interplay coordinates spindle assembly in human oocytes. *Nat Commun* 2019; 10:4651.
16. Zamboni L, Thompson RS, Smith DM. Fine morphology of human oocyte maturation in vitro. *Biol Reprod* 1972; 7:425–457.
17. Sathananthan HA. Maturation of the human oocyte in vitro: Nuclear events during meiosis (an ultrastructural study). *Gamete Res* 1985; 12:237–254.
18. Sundström P, Nilsson BO, Liedholm P, Larsson E. Ultrastructure of maturing human oocytes. *Ann N Y Acad Sci* 1985; 442:324–331.
19. Szöllösi D, Mandelbaum J, Plachot M, Salat-Baroux J, Cohen J. Ultrastructure of the human preovulatory oocyte. *J In Vitro Fert Embryo Transf* 1986; 3:232–242.
20. Suzuki S, Kitai H, Tojo R, Seki K, Oba M, Fujiwara T, Iizuka R. Ultrastructure and some biologic properties of human oocytes and granulosa cells cultured in vitro. *Fertil Steril* 1981; 35:142–148.
21. Motta PM, Nottola SA, Micara G, Familiari G. Ultrastructure of human unfertilized oocytes and polyspermic embryos in an IVF-ET program. *Ann N Y Acad Sci* 1988; 541:367–383.
22. Yang YJ, Zhang YJ, Li Y. Ultrastructure of human oocytes of different maturity stages and the alteration during in vitro maturation. *Fertil Steril* 2009; 92:396.e1–396.e6.
23. Nottola SA, Cotichio G, Sciajno R, Gambardella A, Maione M, Scaravelli G, Bianchi S, Macchiarelli G, Borini A. Ultrastructural markers of quality in human mature oocytes vitrified using cryoleaf and cryoloop. *Reprod Biomed Online* 2009; 19:17–27.
24. Shahedi A, Hosseini A, Khalili MA, Norouzi M, Salehi M, Piriaei A, Nottola SA. The effect of vitrification on ultrastructure of human in vitro matured germinal vesicle oocytes. *Eur J Obstet Gynecol Reprod Biol* 2013; 167:69–75.
25. Cotichio G, Dal Canto M, Fadini R, Mignini Renzini M, Guglielmo MC, Miglietta S, Palmerini MG, Macchiarelli G, Nottola SA. Ultrastructure of human oocytes after in vitro maturation. *Mol Hum Reprod* 2016; 22:110–118.
26. Segovia Y, Victory N, Peinado I, García-Valverde LM, García M, Aizpurua J, Monzó A, Gómez-Torres MJ. Ultrastructural characteristics of human oocytes vitrified before and after in vitro maturation. *J Reprod Dev* 2017; 63:377–382.
27. Holubcová Z, Kyjovská D, Martonová M, Páralová D, Klenková T, Kloudová S. Human egg maturity assessment and its clinical application. *J Vis Exp* 2019; 150:e60058. doi: 10.3791/60058.
28. Schindelin J, Arganda-Carreras I, Frise E, Kaynig V, Longair M, Pietzsch T, Preibisch S, Rueden C, Saalfeld S, Schmid B, Tinevez J-Y, White DJ et al. Fiji: An open-source platform for biological-image analysis. *Nat Methods* 2012; 9:676–682.
29. Otsuki J, Nagai Y. A phase of chromosome aggregation during meiosis in human oocytes. *Reprod Biomed Online* 2007; 15:191–197.
30. Mehlmann LM, Terasaki M, Jaffe LA, Kline D. Reorganization of the endoplasmic reticulum during meiotic maturation of the mouse oocyte. *Dev Biol* 1995; 170:607–615.
31. FitzHarris G, Marangos P, Carroll J. Changes in endoplasmic reticulum structure during mouse oocyte maturation are controlled by the cytoskeleton and cytoplasmic dynein. *Dev Biol* 2007; 305:133–144.
32. Yu Y, Dumollard R, Rossbach A, Lai FA, Swann K. Redistribution of mitochondria leads to bursts of ATP production during spontaneous mouse oocyte maturation. *J Cell Physiol* 2010; 224:672–680.
33. Sathananthan AH. Ultrastructural changes during meiotic maturation in mammalian oocytes: Unique aspects of the human oocyte. *Microsc Res Tech* 1994; 27:145–164.
34. Longo FJ, Chen DY. Development of cortical polarity in mouse eggs: Involvement of the meiotic apparatus. *Dev Biol* 1985; 107:382–394.

35. Gulyas BJ. Cortical granules of mammalian eggs. *Int Rev Cytol* 1980; 63:357–392.
36. Sathananthan AH, Ng SC, Chia CM, Law HY, Edirisinghe WR, Ratnam SS. The origin and distribution of cortical granules in human oocytes with reference to Golgi, nucleolar, and microfilament activity. *Ann N Y Acad Sci* 1985; 442:251–264.
37. Ducibella T, Kurasawa S, Rangarajan S, Kopf GS, Schultz RM. Precocious loss of cortical granules during mouse oocyte meiotic maturation and correlation with an egg-induced modification of the zona pellucida. *Dev Biol* 1990; 137:46–55.
38. Otsuki J, Nagai Y, Chiba K. Lipofuscin bodies in human oocytes as an indicator of oocyte quality. *J Assist Reprod Genet* 2007; 24:263–270.
39. Liu J, Lu G, Qian Y, Mao Y, Ding W. Pregnancies and births achieved from in vitro matured oocytes retrieved from poor responders undergoing stimulation in in vitro fertilization cycles. *Fertil Steril* 2003; 80:447–449.
40. Shu Y, Gebhardt J, Watt J, Lyon J, Dasig D, Behr B. Fertilization, embryo development, and clinical outcome of immature oocytes from stimulated intracytoplasmic sperm injection cycles. *Fertil Steril* 2007; 87:1022–1027.
41. Piqueras P, Gallardo M, Hebles M, Jiménez JM, Migueles B, Montero L, Sánchez-Martín F, Sánchez-Martín P. Live birth after replacement of an embryo obtained from a spontaneously in vitro matured metaphase-I oocyte. *Syst Biol Reprod Med* 2017; 63:209–211.
42. Holubcová Z, Kyjovská D, Martonová M, Páralová D, Klenková T, Otevřel P, Štěpánová R, Kloudová S, Hampl A. Egg maturity assessment prior to ICSI prevents premature fertilization of late-maturing oocytes. *J Assist Reprod Genet* 2019; 36:445–452.
43. Gu NH, Zhao WL, Wang GS, Sun F. Comparative analysis of mammalian sperm ultrastructure reveals relationships between sperm morphology, mitochondrial functions and motility. *Reprod Biol Endocrinol* 2019; 17:66.
44. Beuchat A, Thévenaz P, Unser M, Ebner T, Senn A, Urner F, Germond M, Sorzano COS. Quantitative morphometrical characterization of human pronuclear zygotes. *Hum Reprod* 2008; 23:1983–1992.
45. Tesarik J, Martinez F, Rienzi L, Ubaldi F, Iacobelli M, Mendoza C, Greco E. Microfilament disruption is required for enucleation and nuclear transfer in germinal vesicle but not metaphase II human oocytes. *Fertil Steril* 2003; 79:677–681.
46. Zhang J. Revisiting germinal vesicle transfer as a treatment for aneuploidy in infertile women with diminished ovarian reserve. *J Assist Reprod Genet* 2015; 32:313–317.
47. Reznichenko AS, Huyser C, Pepper MS. Mitochondrial transfer: Implications for assisted reproductive technologies. *Appl Transl Genom* 2016; 11:40–47.
48. Koch GL. The endoplasmic reticulum and calcium storage. *Bioessays* 1990; 12:527–531.
49. Sá R, Cunha M, Silva J, Luís A, Oliveira C, Teixeira da Silva J, Barros A, Sousa M. Ultrastructure of tubular smooth endoplasmic reticulum aggregates in human metaphase II oocytes and clinical implications. *Fertil Steril* 2011; 96:143–9.e7.
50. Motta PM, Nottola SA, Makabe S, Heyn R. Mitochondrial morphology in human fetal and adult female germ cells. *Hum Reprod* 2000; 15:129–147.
51. Youle RJ, van der Blik AM. Mitochondrial fission, fusion, and stress. *Science* 2012; 337:1062–1065.
52. de Paula WB, Agip AN, Missirlis F, Ashworth R, Vizcay-Barrena G, Lucas CH, Allen JF. Female and male gamete mitochondria are distinct and complementary in transcription, structure, and genome function. *Genome Biol Evol* 2013; 5:1969–1977.
53. Dvořák M, Tesarik J, Pilka L, Trávník P. Fine structure of human two-cell ova fertilized and cleaved in vitro. *Fertil Steril* 1982; 37:661–667.
54. Pereda J, Croxatto HB. Ultrastructure of a seven-cell human embryo. *Biol Reprod* 1978; 18:481–489.
55. Mohr LR, Trounson AO. Comparative ultrastructure of hatched human, mouse and bovine blastocysts. *J Reprod Fertil* 1982; 66:499–504.
56. Gardner DK, Lane M, Stevens J, Schoolcraft WB. Noninvasive assessment of human embryo nutrient consumption as a measure of developmental potential. *Fertil Steril* 2001; 76:1175–1180.
57. Cho YM, Kwon S, Pak YK, Seol HW, Choi YM, Park DJ, Park KS, Lee HK. Dynamic changes in mitochondrial biogenesis and antioxidant enzymes during the spontaneous differentiation of human embryonic stem cells. *Biochem Biophys Res Commun* 2006; 348:1472–1478.
58. Tobias IC, Khazaei R, Betts DH. Analysis of mitochondrial dimensions and cristae structure in pluripotent stem cells using transmission electron microscopy. *Curr Protoc Stem Cell Biol* 2018; 47:e67.
59. Uraji J, Scheffler K, Schuh M. Functions of actin in mouse oocytes at a glance. *J Cell Sci* 2018; 131:jcs218099.
60. Duan X, Sun SC. Actin cytoskeleton dynamics in mammalian oocyte meiosis. *Biol Reprod* 2019; 100:15–24.
61. Holubcová Z, Howard G, Schuh M. Vesicles modulate an actin network for asymmetric spindle positioning. *Nat Cell Biol* 2013; 15:937–947.
62. Aida T, Oda S, Awaji T, Yoshida K, Miyazaki S. Expression of a green fluorescent protein variant in mouse oocytes by injection of RNA with an added long poly(A) tail. *Mol Hum Reprod* 2001; 7:1039–1046.
63. Sousa Martins JP, Liu X, Oke A, Arora R, Franciosi F, Viville S, Laird DJ, Fung JC, Conti M. DAZL and CPEB1 regulate mRNA translation synergistically during oocyte maturation. *J Cell Sci* 2016; 129:1271–1282.
64. Tetkova A, Susor A, Kubelka M, Nemcova L, Jansova D, Dvoran M, Del Llano E, Holubcova Z, Kalous J. Follicle-stimulating hormone administration affects amino acid metabolism in mammalian oocytes. *Biol Reprod* 2019; 101:719–732.
65. Danev R, Yanagisawa H, Kikkawa M. Cryo-electron microscopy methodology: Current aspects and future directions. *Trends Biochem Sci* 2019; 44:837–848.
66. Briggman KL, Bock DD. Volume electron microscopy for neuronal circuit reconstruction. *Curr Opin Neurobiol* 2012; 22:154–161.
67. Tachibana M, Kuno T, Yaegashi N. Mitochondrial replacement therapy and assisted reproductive technology: A paradigm shift toward treatment of genetic diseases in gametes or in early embryos. *Reprod Med Biol* 2018; 17:421–433.